PhytoMycology

PhytoMycology (2026) 2: 2004
https://doi.org/10.65390/phtomyc.2026.2004

Research Article

OPEN ACCESS

Morphological and molecular analyses reveal three new species and one new record of endophytic fungi from *Rhododendron decorum* in northwestern Yunnan, China

Zi-Yang Huang[1], Hong-Wei Shen[1], Yong-Zhong Lu[2] and Zong-Long Luo[1,3*]

[1]College of Agriculture and Biological Science, Dali University, Dali 671003, China; [2]School of Food and Pharmaceutical Engineering, Guizhou Institute of Technology, Guiyang 550003, China; [3]Co-Innovation Center for Cangshan Mountain and Erhai Lake Integrated Protection and Green Development of Yunnan Province, Dali University, Dali 671003, China

***Corresponding author:** luozonglongfungi@163.com (Z.-L. L)

Received: 23 November 2025 / Accepted: 26 August 2026 / Published: 15 September 2026

Abstract

Northwestern Yunnan is one of the most biodiversity-rich regions in the world. *Rhododendron decorum* is a dominant evergreen shrub or small tree in the subalpine coniferous forests and rhododendron shrublands of this region, playing an important role in maintaining ecosystem functions and serving as a traditional medicinal and edible resource for local communities. During an investigation of the endophytic fungal diversity associated with *R. decorum* in northwestern Yunnan, sixteen fungal strains were isolated and identified using the tissue isolation method, of which fourteen isolates belonged to *Sordariomycetes* and two to *Leotiomycetes*. Based on morphological characteristics and multigene phylogenetic analyses, three new species are introduced in this study, *viz*., *Pestalotiopsis decori*, *P. jianchuanensis*, and *Pezicula gaoligongensis*. In addition, *Colletotrichum godetiae* is reported for the first time as an endophyte of *R. decorum*. Although *Trichothecium roseum* has been previously recorded from this host, it is redescribed and illustrated in detail in the present study. These findings contribute to the knowledge of the taxonomic diversity and host associations of endophytic fungi associated with *Rhododendron decorum* in northwestern Yunnan.

Key words: Endophytic fungi, Morphology, Multigene, New species, Phylogeny, *Rhododendron*, Taxonomy

Citation: Huang, Z.-Y., Shen, H.-W., Lu, Y.-Z., Luo, Z.-L. (2026) Morphological and molecular analyses reveal three new species and one new record of endophytic fungi from *Rhododendron decorum* in northwestern Yunnan, China. PhytoMycology (2026) 2: 2004 https://doi.org/10.65390/phytomyc.2026.2004

Introduction

Rhododendron is the largest genus of woody plants in the Northern Hemisphere and the most species-rich genus in Ericaceae (Fang et al. 2005; Shrestha et al. 2018). *Rhododendron decorum* is widely distributed across northwestern Yunnan, western Sichuan, and eastern Xizang, occurring at elevations of 1,800–4,000 m (Tian et al. 2011). As a dominant evergreen shrub or small tree at the edges of montane forests and in alpine shrublands, *R. decorum* plays an important role in maintaining habitat structure, promoting soil stability, and supporting biodiversity (Zhang et al. 2021). In addition, its large and fragrant flowers make it a valuable ornamental species, while its traditional use as both a medicinal and edible plant underscores its cultural and economic importance in southwestern China (Wang et al. 2013; Zhu et al. 2019).

Given the ecological, ornamental, and ethnobotanical importance of *Rhododendron* (Ericaceae), it is crucial to study and document the fungi associated with this host. Among plant-associated microorganisms, endophytic fungi are of particular interest because they inhabit healthy plant tissues without causing apparent disease symptoms and typically establish mutualistic associations with their hosts (Petrini & Fisher 1990; Saikkonen et al. 1998, 2004). These fungi play important ecological roles by promoting host growth, enhancing resistance to biotic and abiotic stresses, and protecting against pathogen invasion (Gao et al. 2010; Fontana et al. 2021; Poveda et al. 2021). In addition, many endophytic fungi are capable of synthesizing bioactive secondary metabolites, including compounds that are identical or structurally similar to those of their host, which have been demonstrated to possess antibacterial, antitumor, and antiviral activities (Zhao et al. 2011; Kusari et al. 2013; Meena et al. 2019). This remarkable metabolic capacity renders endophytic fungi a promising microbial resource for drug discovery and the sustainable utilization of medicinal plants. Moreover, endophytic fungi exhibit considerable ecological plasticity, being able to shift among mutualistic, saprotrophic, and pathogenic lifestyles depending on host conditions and environmental factors (Promputtha et al. 2007;

De Silva et al. 2017), thereby contributing to plant health and nutrient cycling.

Northwestern Yunnan, located on the southeastern margin of the Qinghai–Xizang Plateau and within the core area of the "Three Parallel Rivers" region of the Hengduan Mountains, it is characterized by unique geology, complex topography, and diverse climatic conditions, and is widely recognized as one of the most biodiversity-rich regions in the world (Sun et al. 2017; UNESCO World Heritage Centre 2025). These conditions have fostered highly heterogeneous habitats that support exceptionally high plant diversity, with Ericaceae being particularly well represented. Among them, *R. decorum* is a dominant evergreen shrub or small tree in subalpine coniferous forests and rhododendron thickets, playing an important role in maintaining ecosystem functions, while also serving as a traditional medicinal and edible resource for local communities (Tian et al. 2011; Georgian & Emshwiller 2016). In these high-altitude environments, endophytic fungi associated with *R. decorum* may have co-evolved with their host, forming unique interactions that enhance host nutrient acquisition, stress tolerance, and pathogen defense (Schardl et al. 2008; Tian et al. 2011). However, systematic studies on the diversity of endophytic fungi associated with *R. decorum* in northwestern Yunnan are still very limited.

As part of the investigation into the diversity of endophytic fungi associated with *R. decorum* in northwestern Yunnan, China, 16 fungal strains were isolated and identified from fresh healthy leaves. These strains belong to the families *Dermateaceae*, *Glomerellaceae*, *Myrotheciomycetaceae*, and *Pestalotiopsidaceae*. Based on morphological characteristics and multigene phylogenetic analyses, three novel species, *Pestalotiopsis decori*, *P. jianchuanensis*, and *Pezicula gaoligongensis* are described herein, along with one new host record *Colletotrichum godetiae*, and one known species, *Trichothecium roseum*. Detailed descriptions and illustrations of these species are provided. These findings not only enrich our understanding of the endophytic fungal diversity associated with *R. decorum* in northwestern Yunnan, but also provide valuable references for the conservation and utilization of these fungi. Furthermore, all isolated strains have been preserved as resources for future studies on their secondary metabolites and functional properties.

Materials and methods

Sample collection, isolation and morphology

After recording important field information (Rathnayaka et al. 2024), fresh and healthy leaves of *R. decorum* were collected from the northwest of Yunnan Province, China (Table 1). The leaves were placed in a sterile polyethylene bag and stored at 4 °C. The symptomless and mature leaves of *R. decorum* were rinsed with gently running tap water to remove the surface debris. Surface sterilization and inoculation were performed on a clean laminar flow bench. They were surface-sterilized using 75% ethanol for 1 min, followed by treatment with 0.1% $HgCl_2$ for 3 min, rinsed five times with sterilized distilled water, and subsequently dried on sterile filter paper (Tao et al. 2013; Gu et al. 2022). To confirm sterilization efficiency, aliquots of the final rinse water were plated onto potato dextrose agar (PDA) as negative controls. Leaf discs (5 mm in diameter) treated as above were placed on PDA plates with antibiotics. The PDA plates were incubated in ambient light at 25 °C. Once colonies appeared, they were transferred onto fresh PDA plates for further incubation at 25 °C in ambient light for morphological examination.

Macromorphological characters of conidiomata produced on PDA were observed using an Optec SZ 760 stereomicroscope. A Nikon ECLIPSE Ni-U compound microscope was used to observe microscope slides mounted with spore suspension and to capture micromorphological characters. The sporulated culture was placed onto a water-agar medium (WA) containing glycerol and air-dried at room temperature (De Silva et al. 2019). Specimens were deposited in the Herbarium of Cryptogams Kunming Institute of Botany, Academia Sinica (KUN-HKAS), Kunming, China. Living cultures were deposited in the China General Microbiological Culture Collection Center (CGMCC), Beijing, China, and the Kunming Institute of Botany Culture Collection Center (KUNCC), Kunming, China. The Fungal Name number (FN) of the new species was registered (Fungal Names). New species were established following the recommendations outlined in Chethana et al. (2021).

Table 1. Sampling sites of *Rhododendron decorum* leaves in northwestern Yunnan, China

Sample sites	Longitude (°E)	Latitude (°N)	Elevation (m)	Date
Jianchuan County	99°54′15.23″	26°31′53.02″	2713	2023.10.22
Yulong Snow Mountain	100°10′59.75″	26°57′21.75″	3037	2024.09.26
Weixi County	99°21′35.24″	27°00′45.96″	2475	2024.09.26
Gongshan County	98°36′22.80″	28°01′08.22″	1794	2024.09.28
Gaoligong Mountain	98°44′42.03″	25°58′2.95″	2792	2024.04.04

DNA extraction, PCR amplification and sequencing

The Trelief™ Plant Genomic DNA Kit (TSP101-50) was used to extract DNA from fresh mycelium growing on PDA at 25 °C (Beijing Tsingke Biological Engineering Technology and Services Co., Ltd, Beijing, P.R. China). Nine gene regions (ITS, LSU, *tef*1-α, *act*, *chs*1, *gapdh*, *rpb*2, *his*3, and *tub*2) were amplified using the following primer pairs: ITS5/ITS4 (White et al. 1990), LR0R/LR5 (Vilgalys & Hester 1990), EF1-728F/EF2 (Carbone & Kohn 1999), Act-512F/Act-783R (Carbone & Kohn 1999), CHS-79F/CHS-345R (Carbone & Kohn 1999), GDR1/GDF1 (Templeton et al. 1992), fRPB2-5F2/fRPB2-7cR (Liu et al. 1999), CYLH3F/CYLH3R (Crous et al. 2004), and Bt2a/Bt2b (Glass & Donaldson 1995).The PCR reaction mixture had a total volume of 25 μL, containing 12.5 μL 2× Taq PCR Master Mix with blue dye (Sangon Biotech, China), 1 μL of each primer (10 μM), 1 μL of genomic DNA, and 9.5 μL deionized water (Wang et al. 2019). PCR amplification conditions followed the protocols described by Damm et al. (2012) and Gu et al. (2022). Amplifications were verified on 1%

agarose electrophoresis gel stained with ethidium bromide. The resulting PCR amplicons were purified and sequenced at Tsingke Biological Engineering Technology and Services Company, Yunnan, China.

Phylogenetic Analyses

Sequences were subjected to BLAST searches in NCBI (NCBI, accessed on 7 June 2025) using the BLASTn algorithm. Consensus and reference sequences were automatically aligned using MAFFT v.7 (MAFFT Server, accessed on 7 June 2025) (Kuraku et al. 2013; Katoh et al. 2019), and trimmed using trimAl v1.2 with default settings (trimAl, Capella-Gutiérrez et al. 2009). Aligned sequences of each gene region were combined using BioEdit v.7.0.5.2 (Hall 1999). FASTA alignment formats were converted to PHYLIP and NEXUS formats using the ALignment Transformation EnviRonment (ALTER) (ALTER, accessed on 7 June 2025, Glez-Peña et al. 2010). Maximum likelihood (ML) and Bayesian inference (BI) methods were employed to conduct phylogenetic analyses.

Maximum likelihood analysis was performed in the CIPRES Science Gateway v.3.3 (Miller et al. 2010) using RAxML-HPC2 on ACCESS (Stamatakis et al. 2006, 2008). The optimal ML tree search was conducted with 1,000 independent runs using the default algorithm of the program, starting from a random tree for each run. The final tree was selected from the suboptimal trees generated during each run by comparing their likelihood scores using the GTRGAMMA+I substitution model. Bootstrap support values equal to or greater than 75% were given as the first set of numbers above the nodes in the resulting ML tree.

Bayesian inference analysis was performed using MrBayes v.3.1.2 (Ronquist & Huelsenbeck 2003). The model for each gene was estimated using MrModeltest 2.3 (Nylander 2004). Posterior probabilities (PP) (Rannala & Yang 1996) were estimated through Markov chain Monte Carlo (MCMC) sampling in MrBayes v.3.1.2 (Liu et al. 2012). Phylogenetic trees were visualized using FigTree v.1.4.0 (http://tree.bio.ed.ac.uk/software/figtree/), with editing and typesetting performed in Adobe Illustrator (AI) (Adobe Systems Inc., San Jose, CA, USA). New sequences have been deposited in GenBank, and their accession numbers are provided in Supplementary Tables S1–S4.

Results

Phylogenetic analyses

The phylogenetic topology of *Pestalotiopsis* was inferred from a combined dataset of ITS, *tef*1-α, and *tub*2 sequences, comprising 253 *Pestalotiopsis* isolates and one outgroup taxa (*Neopestalotiopsis cubana* CBS 600.96), with a total of 2,137 characters including gaps (ITS: 1–528 bp; *tef*1-α: 529–1452 bp; *tub*2: 1453–2137 bp). Phylogenetic analyses showed that the six newly obtained strains (CGMCC 3.29126, KUNCC 23-16940, KUNCC 23-16941, CGMCC 3.29129, CGMCC 3.29130 and KUNCC 25-19536) clustered with *P. ericacearum* (IFRDCC 2439) with 100% ML and 1.00 PP support (Fig. 1). In addition, two strains (KUNCC 23-16950 and KUNCC 23-16961) clustered with *P. rosarioides* (CGMCC 3.23549), *P. intermedia* (MFLUCC 12-0259), and *P. linearis* (MFLUCC 12-0271) to form an independent clade (Fig. 1).

The phylogenetic topology of *Pezicula* was inferred from a combined dataset of ITS, LSU, and *rpb*2 sequences, comprising 53 *Pezicula* strains and two outgroup taxa (*Parafabraea caliginosa* CBS 124806 and *P. eucalypti* CBS 124810), with 2,340 characters including gaps (ITS: 1–547 bp; LSU: 548–1294 bp; *rpb*2: 1295–2340 bp). Phylogenetic analyses showed that our strains (CGMCC 3.29135 and KUNCC 24-18741) clustered with *P. neosporulosa* (CBS 101.96 and CBS 102.96) with 0.97 PP support (Fig. 2).

The phylogenetic topology of *Colletotrichum* was inferred from a combined dataset of ITS, *act*, *chs*1, *gapdh*, *his*3, and *tub*2 sequences, comprising 72 *Colletotrichum* strains and one outgroup taxa (*Colletotrichum orchidophilum* CBS 632.80), with 2,181 characters including gaps (ITS: 1–537 bp; *act*: 538–783 bp; *chs*1: 784–1063 bp; *gapdh*: 1064–1310 bp; *his*3: 1311–1692 bp; *tub*2: 1693–2181 bp). The RAxML and BI analyses of the combined dataset resulted in similar topologies. Phylogenetic analyses showed that the five newly obtained strains of *Colletotrichum godetiae* (CGMCC 3.29136, CGMCC 3.29137, CGMCC 3.29138, CGMCC 3.29139 and CGMCC 3.29140) clustered with its ex-type strain with 94% ML and 1.00 PP support and are located in the *C. acutatum* species complex (Fig. 3).

The phylogenetic topology of *Trichothecium* was inferred from a combined dataset of ITS and LSU sequences, comprising 28 *Trichothecium* strains and one outgroup taxa (*Passalora fulva* EAV), with 1,066 characters including gaps (ITS: 1–509 bp; LSU: 510–1066 bp). Phylogenetic analyses showed that our *Trichothecium roseum* strain (CGMCC 3.29134) clustered with its type strain with 86% ML support (Fig. 4).

Taxonomy

Pestalotiopsis decori Z.Y. Huang, H.W. Shen & Z.L. Luo, sp. nov., Figure 5.

Fungal Names number: FN 572994.

Holotype: —HKAS 136937

Etymology: — "*decori*" refers to the host plant *Rhododendron decorum*, which the fungus was isolated.

Endophytic in healthy *Rhododendron decorum* leaves. **Sexual morph:** Undetermined. **Asexual morph:** *Conidiomata* in culture sporodochial, saucer-shaped, scattered or gregarious, superficial to immersed, shining, releasing black conidial masses on the surface. *Conidiophores* branched, subcylindrical, hyaline to light brown, indistinct, often reduced to conidiogenous cells. *Conidiogenous cells* cylindrical or ampulliform, hyaline, smooth-walled, solitary to aggregated, (12–22 × 3.5–5.5 µm) ($\bar{x}$ = 17 × 4.5 µm, n = 30). Conidia 23–29 × 7–9 µm ($\bar{x}$= 26 × 8 µm, n = 30), fusoid, ellipsoid, rosary, straight to slightly curved, four-septate; basal cell conic with a truncated base, hyaline or light brown, and thin-walled, 4–6 µm long ($\bar{x}$ = 5 µm, n = 30); three-median cells dark,17–19 µm long ($\bar{x}$ = 18 µm, n = 30), smooth wall, concolourous, septa darker than the rest of the cells (second cell from the base pale brown and enlarged, 5–6 µm long; third cell 5–7 µm long; fourth cell expands to 6–7 µm long); apical cell 5–7 µm long ($\bar{x}$ = 6 µm, n = 30), hyaline, subcylindrical, thin and smooth-walled, with 2–4 tubular apical appendages 30–52 µm long ($\bar{x}$ = 41 µm, n = 30) arising from the apical crest, unbranched, filiform; basal appendage

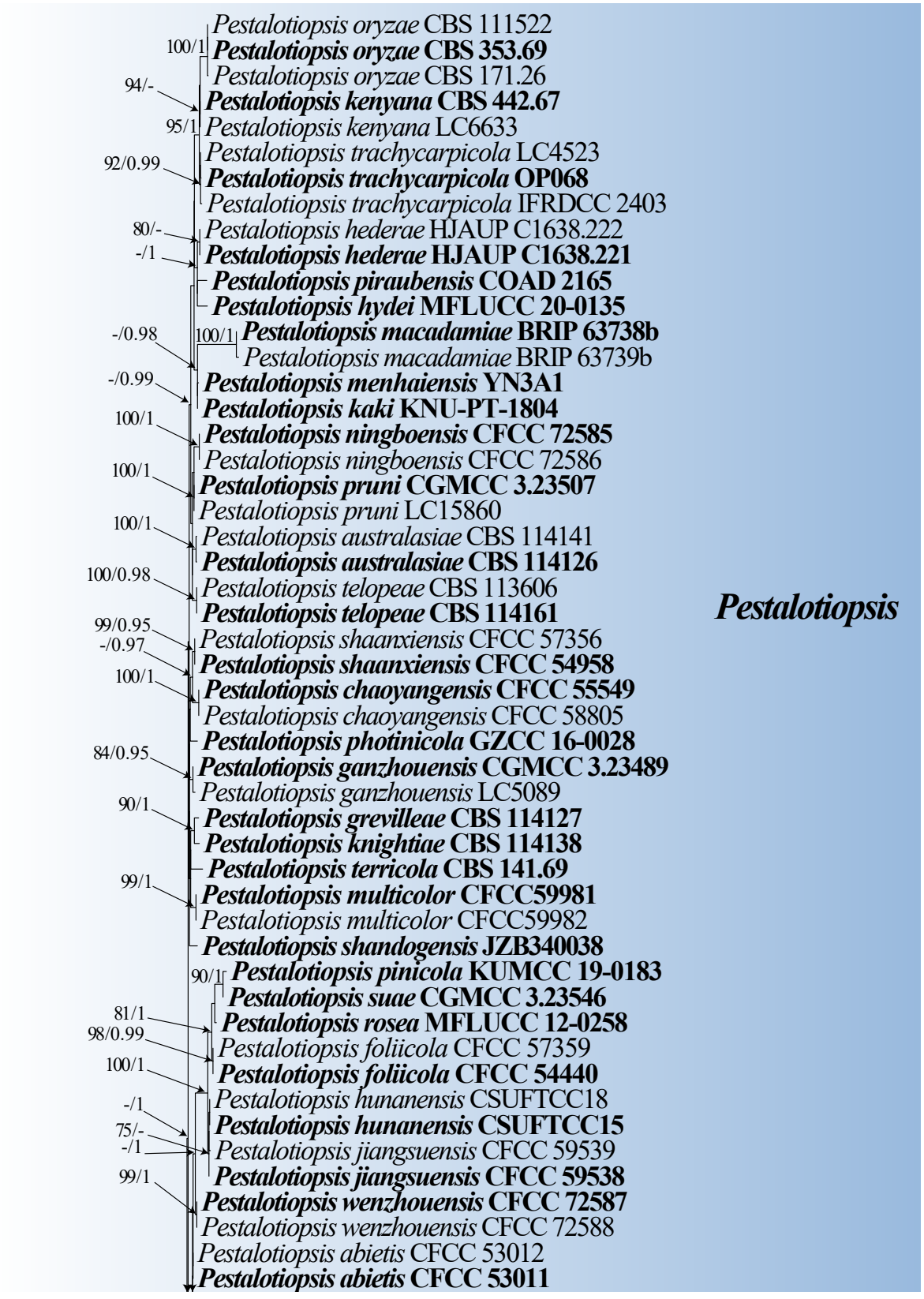

Fig 1. Maximum likelihood tree based on the analysis of combined ITS, *tef*1-α, and *tub*2 dataset. The tree is rooted to *Neopestalotiopsis cubana* (CBS 600.96). The RAxML and BI analyses of the combined dataset yielded similar topologies. The final likelihood value of ML analysis was -22317.277447. The matrix had 1093 distinct alignment patterns, with 25.98% undetermined characters or gaps. The estimated base frequencies were as follows: A = 0.237126, C = 0.295354, G = 0.215682, T = 0.251839; substitution rates AC = 1.136383, AG = 3.639232, AT = 1.457155, CG = 1.040074, CT = 5.437934, GT = 1.000000; gamma distribution shape parameter α = 0.300713. Bootstrap support values (ML) equal to or greater than 75% and BI posterior probabilities (PP) equal to or higher than 0.95 are given near the nodes as ML/PP. A hyphen represents bootstrap values below 75% for ML and below 0.95 for PP. Ex-type strains are indicated in bold and newly generated sequences are shown in red.

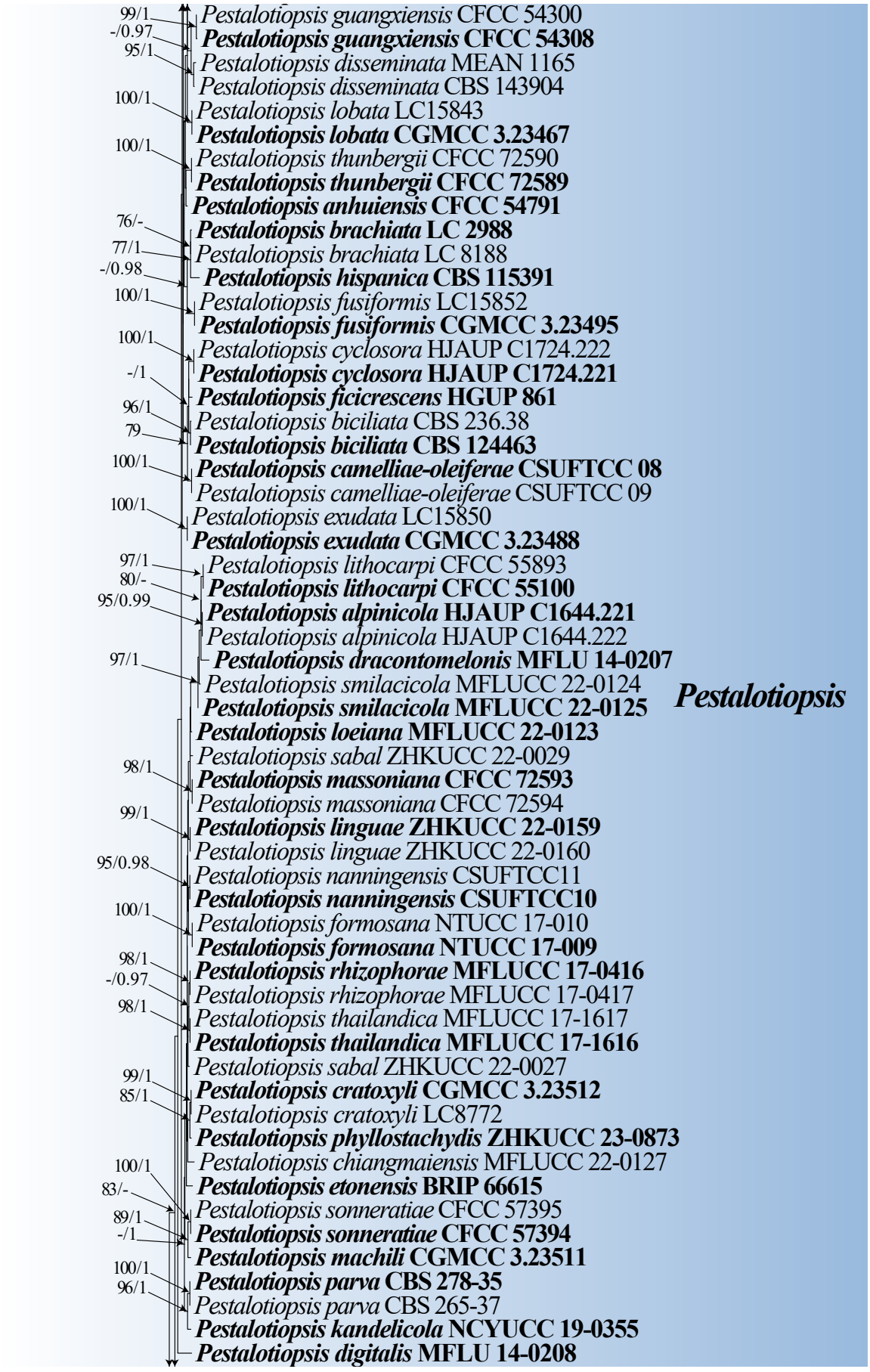

Fig 1. (continued)

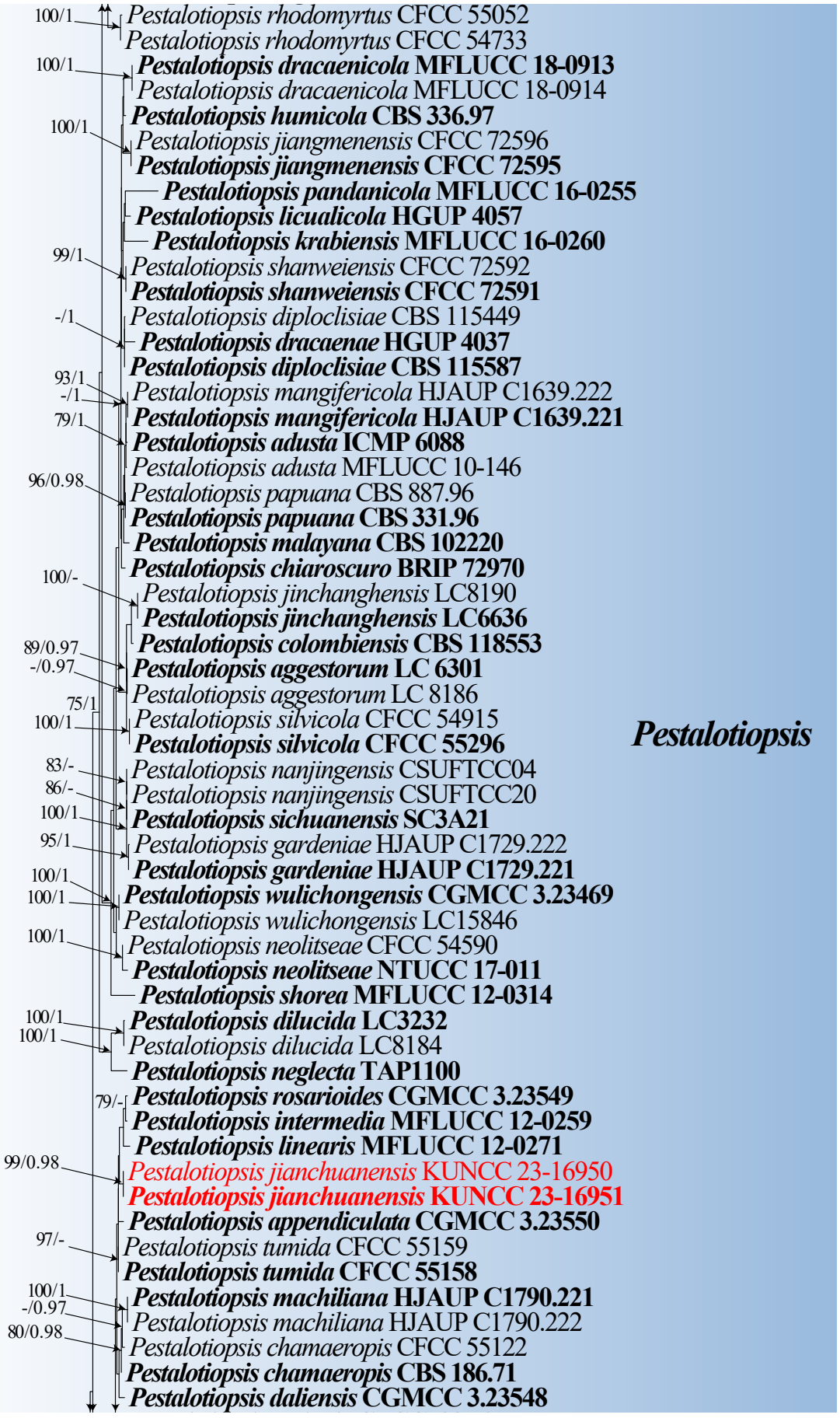

Fig 1. (continued)

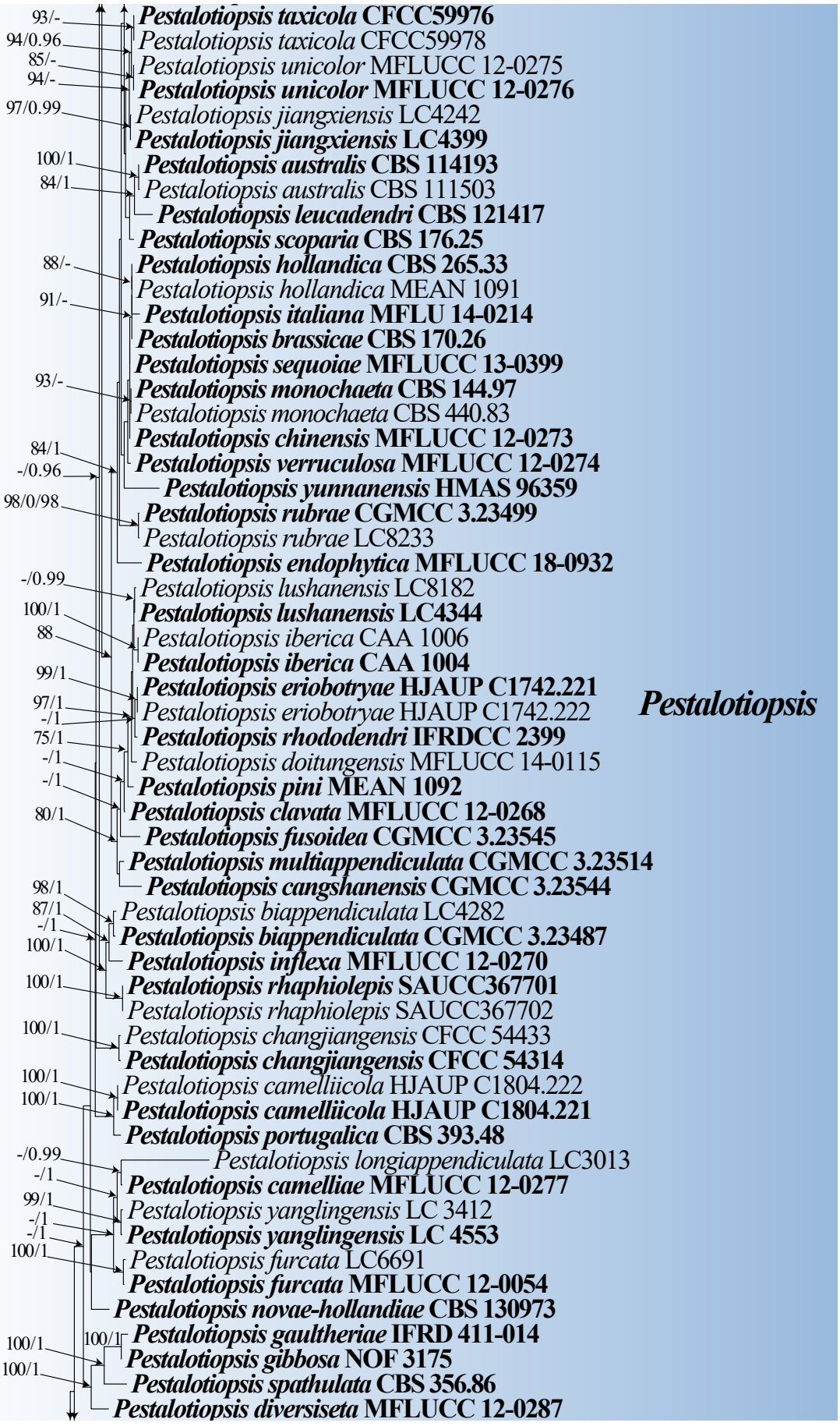

Fig 1. (continued)

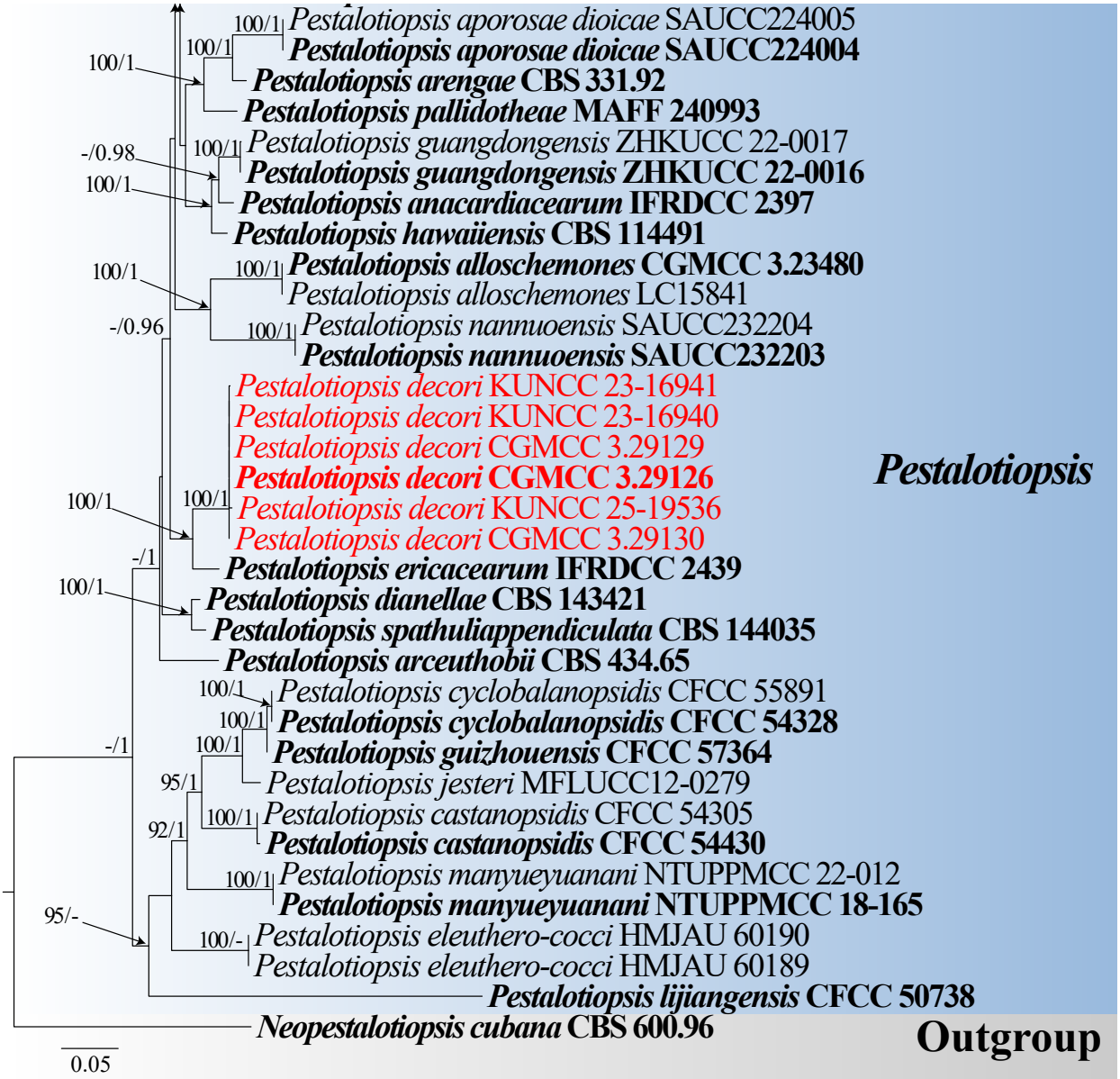

Fig 1. (continued)

8–20 µm long ($\bar{x}$ = 14 µm, n = 30), single, tubular, unbranched, centric, straight, or slightly curved.

Culture characteristics: —Colonies on PDA reaching 30–40 mm diameter after 14 days at 25 °C in darkness. The surface of the colony was white, the aerial hyphae were flocculent, the back was light orange, and the edges were irregular. Black conidiomata are formed after 14 days on PDA.

Material examined: —China, Yunnan Province, Dali City, Jianchuan County, 26°31′53.02″ N, 99°54′15.23″ E (2713 m), isolated from healthy leaves of *R. decorum*, October 2023, Z.Q. Zhang, B-5 (HKAS 136937, holotype), ex-holotype living culture, CGMCC 3.29126 = KUNCC 23-16938; *ibid.*, isolated from healthy leaves of *R. decorum*, October 2023, Z.Q. Zhang, B-7 (HKAS 136938), living culture, KUNCC 23-16940; *ibid.*, isolated from healthy leaves of *R. decorum*, October 2023, Z.Q. Zhang, B-8 (HKAS 136939), living culture, KUNCC 23-16941; *ibid.*, isolated from healthy leaves of *R. decorum*, October 2023, Z.Q. Zhang, B-32 (HKAS 136931), living culture, CGMCC 3.29129 = KUNCC 23-16959; *ibid.*, isolated from healthy leaves of *R. decorum*, October 2023, Z.Q. Zhang, B-33 (HKAS 136936), living culture, CGMCC 3.29130 = KUNCC 23-16960; China, Yunnan Province, Nujiang City, Gongshan County, 28°01′08.22″ N, 98°36′22.80″ E (1794 m), isolated from healthy leaves of *R. decorum*, September 2024, Z.Y. Huang, B-766 (HKAS 148956, paratype), ex-paratype living culture, KUNCC 25-19536.

Notes: —Six newly obtained strains (CGMCC 3.29126, KUNCC 23-16940, KUNCC 23-16941, CGMCC 3.29129, CGMCC 3.29130, and KUNCC 25-19536) of *Pestalotiopsis decori* clustered with *P. ericacearum* (IFRDCC 2439) and formed a well-supported sister clade (100% ML/1.00 PP, Fig. 1). Sequence comparison revealed 57 nucleotide differences between CGMCC 3.29126 and *P. ericacearum* including 9 bp differences in ITS (523 bp), 40 bp differences in *tef*1-α (450 bp), and 8 bp differences in *tub*2 (417 bp). Morphologically, *Pestalotiopsis decori* (HKAS 136937) differs from *P. ericacearum* by its larger conidia (23–29 × 7–9 µm *vs.* 16–20 × 5–9 µm), longer apical appendages (30–52 µm *vs.* 20–43 µm) and basal appendages (8–20 µm *vs.* 2–9 µm) (Zhang et al. 2013). In addition, *P. decori* possesses 2–4 apical appendages,

whereas *P. ericacearum* bears 3–4 (Zhang et al. 2013). Notably, both species were isolated from the leaves of *Rhododendron* species, however, *P. ericacearum* was obtained from *R. delavayi*, whereas our collections were recovered from *R. decorum*.

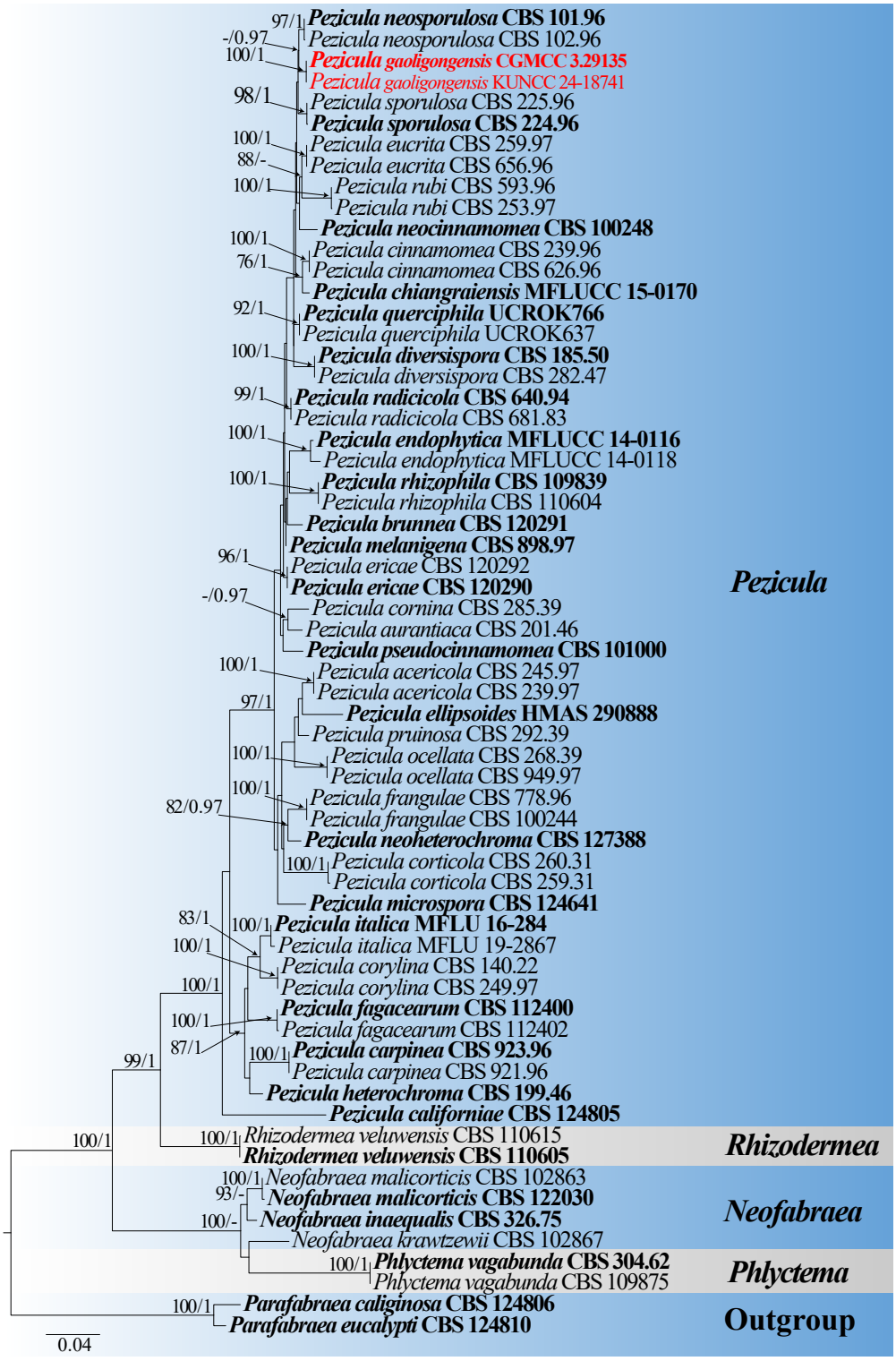

Fig 2. Maximum likelihood tree based on the analysis of combined ITS, LSU, and *rpb2* dataset. The tree is rooted with *Parafabraea caliginosa* (CBS 124806) and *P. eucalypti* (CBS 124810). The RAxML and BI analyses of the combined dataset resulted in similar topologies. The final likelihood value of ML analysis was -11515.987393. The matrix had 674 distinct alignment patterns, with 18.85% undetermined characters or gaps. The estimated base frequencies were as follows: A = 0.247578, C = 0.233945, G = 0.275287, T = 0.243190; substitution rates AC = 1.828907, AG = 4.038639, AT = 0.968650, CG = 0.913467, CT = 10.964282, GT = 1.000000; gamma distribution shape parameter α = 0.145991. Bootstrap support values (ML) equal to or greater than 75% and BI posterior probabilities (PP) equal to or higher than 0.95 are given near the nodes as ML/PP. A hyphen represents bootstrap values below 75% for ML and below 0.95 for PP. Ex-type strains are indicated in bold and newly generated sequences are shown in red.

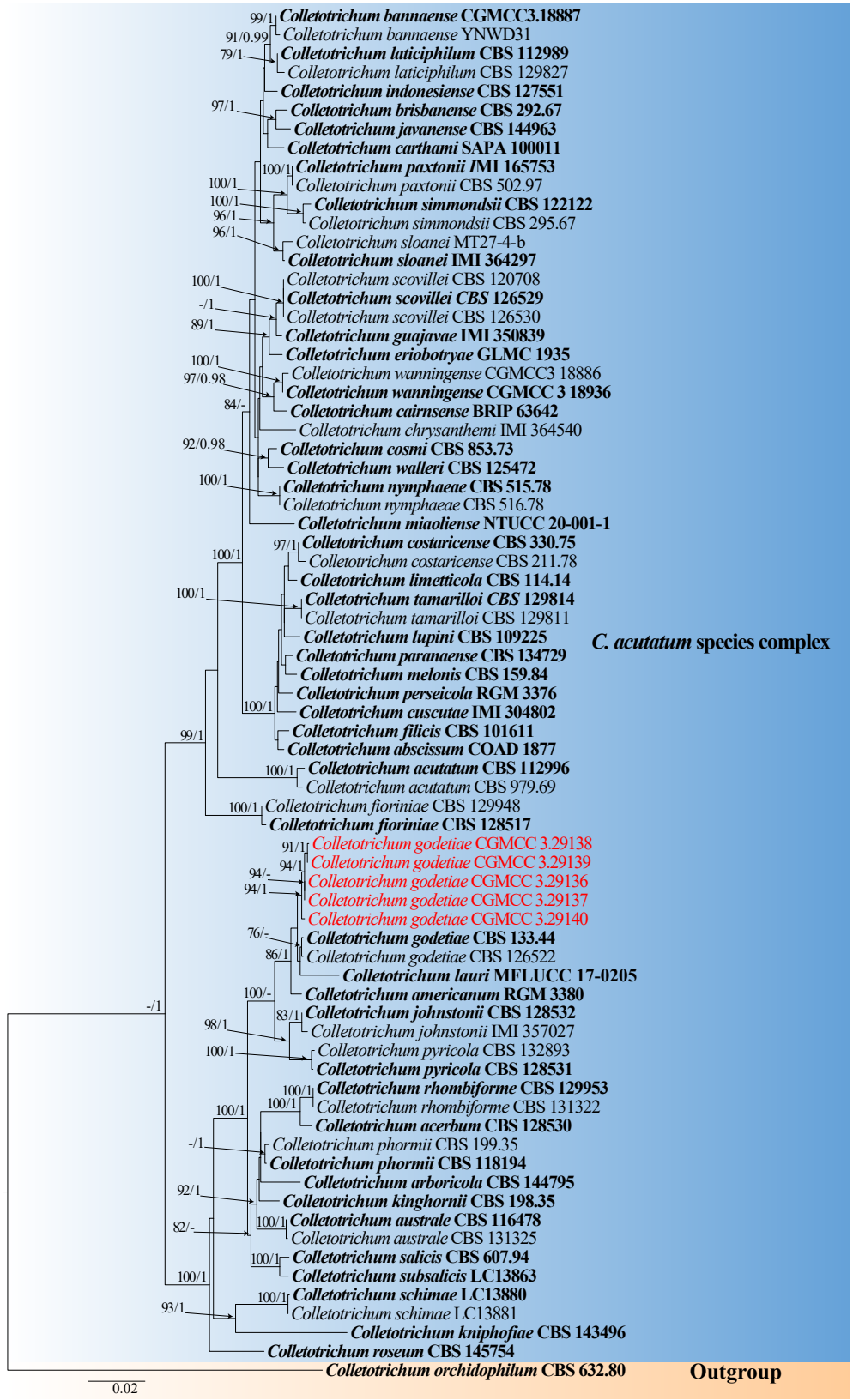

Fig 3. Maximum likelihood tree based on the analysis of combined ITS, *act*, *chs*1, *gapdh*, *his*3, and *tub*2 dataset. The tree is rooted with *Colletotrichum orchidophilum* (CBS 632.80). The final likelihood value of ML analysis was –9928.033775. The matrix had 650 distinct alignment patterns, with 4.19% undetermined characters or gaps. The estimated base frequencies were as follows: A = 0.224070, C = 0.310984, G = 0.239958, T = 0.224988; substitution rates AC = 1.776177, AG = 5.026397, AT = 1.683724, CG = 0.796886, CT = 9.308339, GT = 1.000000; gamma distribution shape parameter α = 0.218374. Bootstrap support values (ML) equal to or greater than 75% and BI posterior probabilities (PP) equal to or higher than 0.95 are given near the nodes as ML/PP. A hyphen represents bootstrap values below 75% for ML and below 0.95 for PP. Ex-type strains are indicated in bold and newly generated sequences are shown in red.

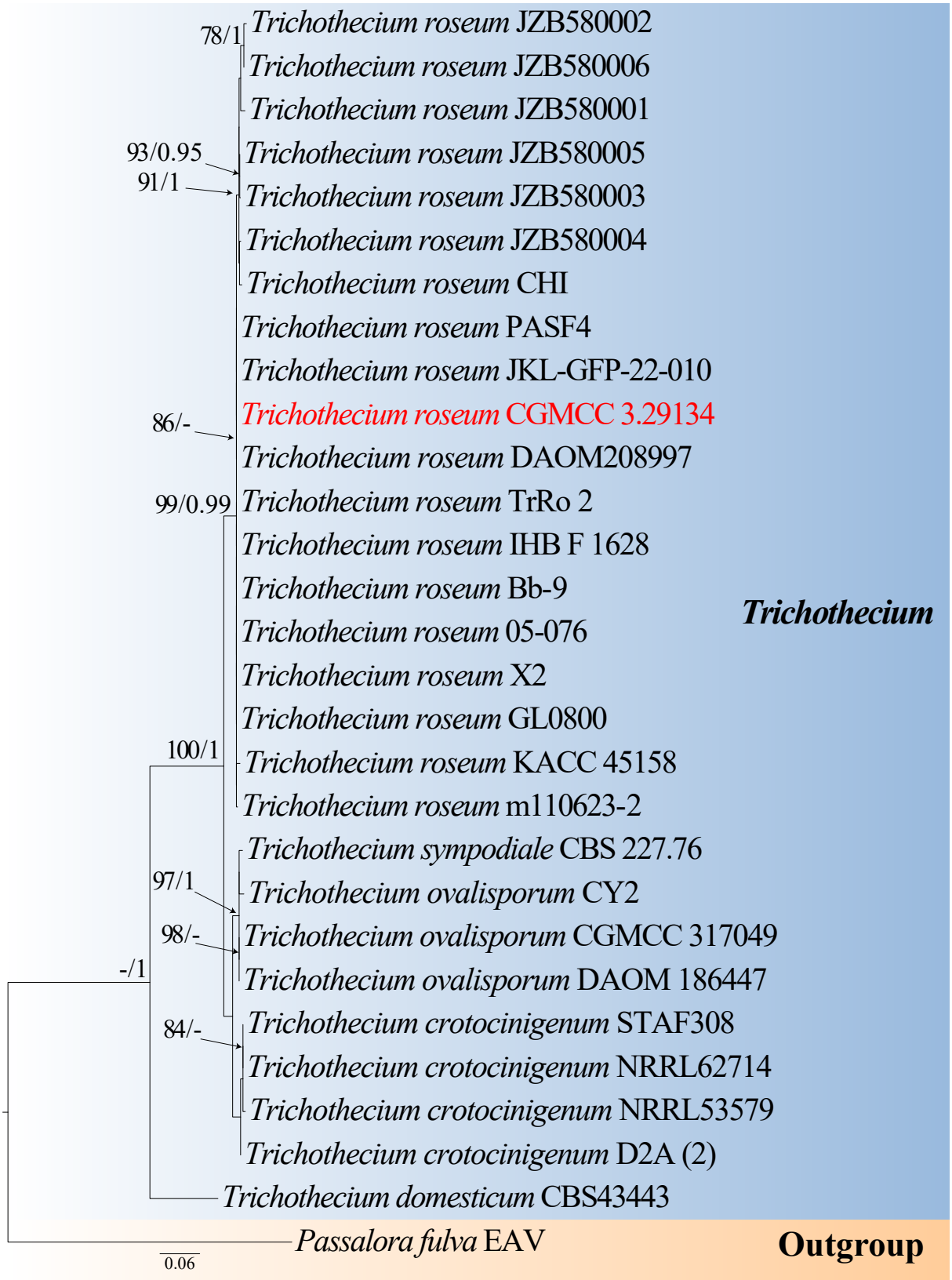

Fig 4. Maximum likelihood tree based on the analysis of combined ITS and LSU dataset. The tree is rooted with *Passalora fulva* (EAV). The RAxML and BI analyses of the combined dataset resulted in similar topologies. The final likelihood value of ML analysis was –2973.594884. The matrix had 156 distinct alignment patterns, with 31.27% undetermined characters or gaps. The estimated base frequencies were as follows: A = 0.224494, C = 0.297200, G = 0.280965, T = 0.197341; substitution rates AC = 1.965073, AG = 2.290962, AT = 1.631854, CG = 1.599496, CT = 5.817759, GT = 1.000000; gamma distribution shape parameter α = 0.420489. Bootstrap support values (ML) equal to or greater than 75% and BI posterior probabilities (PP) equal to or higher than 0.95 are given near the nodes as ML/PP. A hyphen represents bootstrap values below 75% for ML and below 0.95 for PP. Ex-type strains are in bold and newly generated sequence are shown in red.

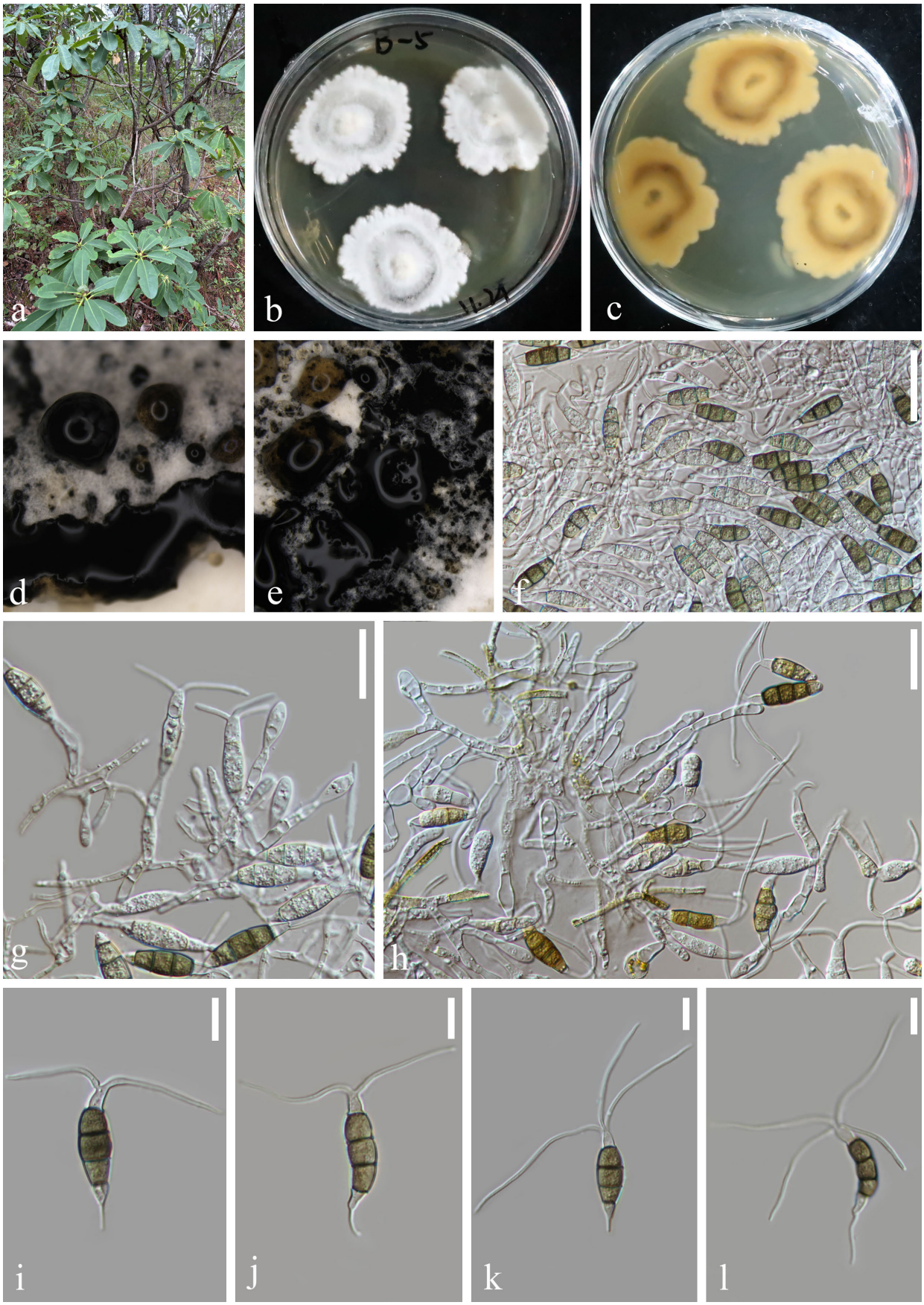

Fig 5. ***Pestalotiopsis decori*** **(HKAS 136937, holotype) a.** Leaves of *Rhododendron decorum*. **b, c.** Culture on potato dextrose agar (PDA) (obverse and reverse view). **d, e.** Conidiomata on PDA. **f–h.** Conidiogenous cells and developing conidia. **i–l.** Conidia. Scale bars: **f** = 30 µm, **g, h** = 20 µm, **i–l** = 10 µm.

Pestalotiopsis jianchuanensis Z.Y. Huang, H.W. Shen & Z.L. Luo, sp. nov., Figure 6.

Fungal Names number: FN 572995.

Holotype: —HKAS 148954

Etymology: — "*jianchuanensis*" refers to Jianchuan County, Yunnan Province, China, where the holotype was collected.

Endophytic in healthy *Rhododendron decorum* leaves. **Sexual morph:** Undetermined. **Asexual morph:** *Conidiomata* (on PDA) pycnidial, globose to clavate, solitary, exuding globose, dark-brown to black conidial masses. *Conidiophores* indistinct and typically reduced to conidiogenous cells. *Conidiogenous cells* cylindrical or ampulliform, hyaline, smooth-walled, solitary to aggregated, (8–14 × 4–12 µm) ($\bar{x}$ = 11 × 8 µm, n = 30). *Conidia* 22–27 × 6–8 µm ($\bar{x}$ = 23 × 7 µm, n = 30), fusoid, ellipsoid, rosary, straight to slightly curved,four-septate; basal cell conic with a truncated base, hyaline or light brown, and thin-walled, 4–6 µm long ($\bar{x}$ = 5 µm, n = 30); three-median cells dark, 14–18 µm long ($\bar{x}$ = 16 µm, n = 30), smooth wall, concolourous, septa darker than the rest of the cells (second cell from the base pale brown and enlarged, 4–5 µm long; third cell 5–6 µm long; fourth cell expands to 5–6 µm long); apical cell 3–5 µm long ($\bar{x}$ = 4 µm, n = 30), hyaline, subcylindrical, thin-walled, and smooth-walled, with 2–3 tubular apical appendages 12–24 µm long ($\bar{x}$ = 18 µm, n = 30) arising from the apical crest, unbranched, filiform; basal appendage 4–8 µm long ($\bar{x}$ = 6 µm, n = 30), single, tubular, unbranched, centric, straight, or slightly curved.

Culture characteristics: —Colonies on PDA reaching 40–60 mm diameter after 14 days at 25 °C in darkness. The surface of the colony was white, the aerial hyphae were flocculent, the back was light orange, and the edges were regular. Black conidiomata are formed after 14 days on PDA.

Material examined: —China, Yunnan Province, Dali City, Jianchuan County, 26°31′53.02″ N, 99°54′15.23″ E (2713 m), isolated from healthy leaves of *R. decorum*, October 2023, Z.Q. Zhang, B-34 (HKAS 148954, holotype), ex-holotype living culture, KUNCC 23-16961; *ibid.*, isolated from healthy leaves of *R. decorum*, October 2023, Z.Q. Zhang, B-18 (HKAS 148959), living culture, KUNCC 23-16950.

Notes: —In the phylogenetic analyses, *Pestalotiopsis jianchuanensis* sp. nov. is closely related to *P. intermedia*, *P. linearis*, and *P. rosarioides* (Fig. 1). Sequence comparisons between *P. jianchuanensis* (KUNCC 23-16961) and related taxa revealed notable nucleotide differences: 19 bp in *tub*2 (342 bp) relative to *P. linearis* (MFLUCC 12-0271); 1 bp, 3 bp, and 8 bp differences in ITS (523 bp), *tef*-1α (549 bp), and *tub*2 (362 bp), respectively, relative to *P. intermedia* (MFLUCC 12-0259); and 4 bp and 3 bp differences in *tef*1-α (406 bp) and *tub*2 (324 bp), respectively, relative to *P. rosarioides* (CGMCC 3.23549). Morphologically, *P. jianchuanensis* can be distinguished from *P. intermedia* and *P. linearis* by its conidial size and appendages characteristics (Table 2). In comparison with *P. rosarioides*, which was also isolated from *R. decorum*, *P. jianchuanensis* can be distinguished by its distinctly longer apical appendages (12–24 µm *vs.* 5–9 µm), longer basal appendages (4–8 µm *vs.* 4–5 µm), and shorter apical cells (3–5 µm *vs.* 4–7 µm) (Gu et al. 2022).

Pezicula gaoligongensis Z.Y. Huang, H.W. Shen & Z.L. Luo, sp. nov., Figure 7.

Fungal Names number: FN 572996.

Holotype: —HKAS 148950

Etymology: — "*gaoligongensis*" refers to the Gaoligong Mountain, where the holotype was collected.

Endophytic in healthy *Rhododendron decorum* leaves. **Sexual morph:** Undetermined. **Asexual morph:** *Conidiomata* erumpent on surface, aggregated or scattered, with brown to black conidial masses, globose to irregular. *Conidiophores* hyaline, cylindrical, straight to flexuous, septate, unbranched or branched, smooth-walled, reduced to conidiogenous cells. *Conidiogenous cells* hyaline, enteroblastic, integrated, smooth-walled. *Conidia* 31–38 × 7–9 µm ($\bar{x}$ = 33 × 8 µm, n = 30), hyaline when young, becoming to pale yellow and eventually to orange-brown with age, elongated ellipsoid to cylindrical, straight or slightly curved, rounded at the apex, narrow and slightly truncate at the base, and with a protruding scar, 2–4-septate, with septa becoming inconspicuous at maturity, granular to guttulate, thin-walled.

Culture characteristics: —Colonies on PDA reaching 40–60 mm diameter after 14 days at 25 °C in darkness. The surface of the colony was white to pale brown, the aerial hyphae were flocculent, the back was brown to white, and the edges were irregular. Brown to black conidiomata developed on PDA after 14 days.

Table 2. Comparison of conidial characteristics and habitats of *Pestalotiopsis jianchuanensis*, *P. intermedia*, *P. linearis*, *P. rosarioides*.

Species	Conidia	Apical cell	Apical appendage	Basal appendage	Host	Country	References
P. jianchuanensis	22–27 × 6–8 µm	3–5 µm	2–3 tubular apical appendages, 12–24 µm	single basal appendage, 4–8 µm	*Rhododendron decorum*	China	This study
P. intermedia	24–28 × 5.5–6.5 µm	4–5 µm	2–3 (rarely 4) tubular apical appendages, 10–28 µm	single basal appendage, 6–10 µm	dead leaf of tree	China	Maharachchikumbura et al. 2012
P. linearis	24–33×4.7–6 µm	4–5 µm	2–3 (rarely 1) tubular apical appendages, 10–20 µm	single (rarely 2) basal appendages, 4–7 µm	*Trachelospermum* sp.	China	Maharachchikumbura et al. 2012
P. rosarioides	22–25 × 6–7 µm	4–7 µm	1–3 tubular apical appendages, 5–9 µm	single basal appendage, 4–5 µm	*Rhododendron decorum*	China	Gu et al. 2022

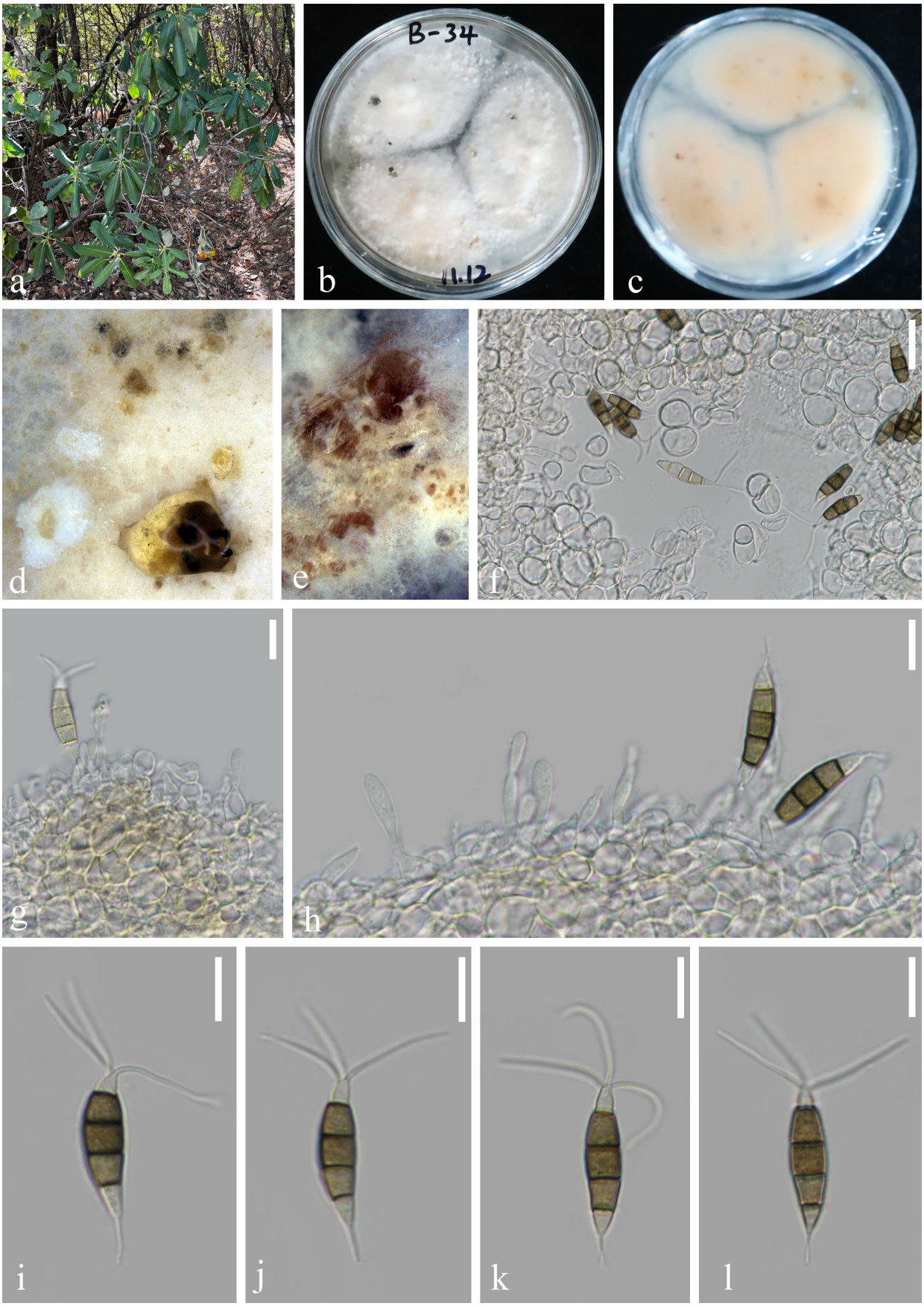

Fig 6. ***Pestalotiopsis jianchuanensis*** **(HKAS 148954, holotype) a.** Leaves of *Rhododendron decorum*. **b, c.** Culture on potato dextrose agar (PDA) (obverse and reverse view). **d, e.** Conidiomata on PDA. **f–h.** Conidiogenous cells and developing conidia. **i–l.** Conidia. Scale bars: **f** = 20 µm, **g–l** = 10 µm.

Fig 7. *Pezicula gaoligongensis* (HKAS 148950, holotype) a. Leaves of *Rhododendron decorum*. **b, c.** Culture on potato dextrose agar (PDA) (obverse and reverse view). **d, e.** Conidiomata on PDA. **f–i.** Conidiogenous cells and developing conidia. **j–l.** Conidia. Scale bars: **f, g, i** = 20 µm, **h** = 10 µm, **j–m** = 15 µm.

Material examined: —China, Yunnan Province, Nujiang City, Gaoligong Mountain, 25°58′2.95″ N, 98°44′42.03″ E (2792 m), isolated from healthy leaves of *R. decorum*, April 2024, R.Z. Ji, B-372 (HKAS 148950, holotype), ex-holotype living culture, CGMCC 3.29135 = KUNCC 24-18742; *ibid.*, isolated from healthy leaves of *R. decorum*, April 2024, R.Z. Ji, B-371 (HKAS 148952), living culture, KUNCC 24-18741.

Notes: —Our two strains of *Pezicula gaoligongensis* (CGMCC 3.29135 and KUNCC 24-18741) clustered together and formed a sister clade to *P. neosporulosa* (CBS 101.96), with 0.97 PP support (Fig. 2). Sequence comparisons revealed 18 bp differences between *P. gaoligongensis* (CGMCC 3.29135) and *P. neosporulosa* (CBS 101.96), including 4 bp in ITS (506 bp), 1 bp in LSU (523 bp), and 13 bp in *rpb*2 (875 bp). Morphologically, *P. gaoligongensis* differs from *P. neosporulosa* by its longer but narrower conidia (31–38 × 7–9 µm *vs.* 20–36.5 × 9–12 µm), and its mature conidia become orange-brown, whereas those of *P. neosporulosa* remain hyaline (Yuan & Verkley 2015). In addition, *P. neosporulosa* produces both macroconidia and microconidia (Yuan & Verkley 2015), whereas this characteristic was not observed in *P. gaoligongensis* (CGMCC 3.29135). Notably, *P. gaoligongensis* was isolated as an endophyte from healthy leaves of *R. decorum*, while *P. neosporulosa* was obtained from *Abies alba* (Yuan & Verkley 2015).

Colletotrichum godetiae Neerg., *Friesia* 4(1-2): 72 (1950), Figure 8.

Endophytic in healthy *Rhododendron decorum* leaves. **Sexual morph:** Undetermined. **Asexual morph:** *Conidiomata* acervular, gregarious, dark brown. *Appressoria* and *Setae* not observed on PDA. *Conidiophores* hyaline, unbranched, approximately cylindrical. *Conidiogenous cells* hyaline, smooth-walled, cylindrical. *Conidia* (15–17 × 4–6 µm) ($\bar{x}$ = 16 × 5 µm, n = 30), hyaline, elongated ellipsoid, straight, aseptate, obtuse at the base, rounded at the apex, smooth-walled, guttulate.

Culture characteristics: —Colonies on PDA reaching 40–70 mm diameter after 14 days at 25 °C in darkness. The surface of the colony was white or gray, the aerial hyphae were flocculent, the back was dark grey to greyish pink, and the edges were irregular. Dark brown conidiomata are formed after 14 days on PDA.

Material examined: —China, Yunnan Province, Lijiang City, Yulong Snow Mountain, 26°57′21.75″ N, 100°10′59.75″ E (3037 m), isolated from healthy leaves of *R. decorum*, September 2024, Z.Y. Huang, B-514 (HKAS 148951), living culture, CGMCC 3.29136 = KUNCC25-19544; *ibid.*, isolated from healthy leaves of *R. decorum*, September 2024, Z.Y. Huang, B-520 (HKAS 148953), living culture, CGMCC 3.29137 = KUNCC 25-19550; *ibid.*, isolated from healthy leaves of *R. decorum*, September 2024, Z.Y. Huang, B-521 (HKAS 148955), living culture, CGMCC 3.29138 = KUNCC 25-19551; *ibid.*, isolated from healthy leaves of *R. decorum*, September 2024, Z.Y. Huang, B-522 (HKAS 148957), living culture, CGMCC 3.29139 = KUNCC 25-19552; China, Yunnan Province, Nujiang City Gongshan County, 28°01′08.22″ N, 98°36′22.80″ E (1794 m), isolated from healthy leaves of *R. decorum*, September 2024, Z.Y. Huang, B-797 (HKAS 148958), living culture, CGMCC 3.29140 = KUNCC 25-19537.

Notes: —Our five strains (CGMCC 3.29136, CGMCC 3.29137, CGMCC 3.29138, CGMCC 3.29139, and CGMCC 3.29140) clustered within the same clade as *Colletotrichum godetiae* and *C. lauri* in the *C. acutatum* species complex (Fig. 3). Sequence comparisons of CGMCC 3.29136 with *C. godetiae* (CBS 133.44) across the ITS, *act*, *chs*1, *gapdh*, *his*3, and *tub*2 regions revealed only minor nucleotide differences (2 bp in *act*, 2 bp in *gapdh*, and 1 bp in *tub*2), whereas comparisons with *C. lauri* (MFLUCC 17-0205) showed substantially greater sequence divergence (1 bp in ITS, 4 bp in *act*, 1 bp in *gapdh*, 6 bp in *chs*1, and 10 bp in *tub*2). In contrast, the morphological characteristics of our isolates are consistent with those of *C. godetiae* (CBS 133.44) (Damm et al. 2012; Hosking et al. 2024). Consequently, we temporarily identified the five strains as *C. godetiae*. This study represents the first report of *C. godetiae* isolated from *Rhododendron decorum*.

Trichothecium roseum (Pers.) Link, *Mag. Gesell. Naturf. Freunde, Berlin* 3(1-2): 18 (1809). Figure 9.

Endophytic in healthy *Rhododendron decorum* leaves. **Sexual morph:** Undetermined. **Asexual morph:** *Colonies* on PDA, superficial, effuse, gregarious, hyaline. *Conidiophores* (124–198 × 2.5–3 µm) ($\bar{x}$ = 161 × 3 µm, n = 15), micronematous, mononematous, cylindrical, septate, hyaline, smooth. *Conidiogenous* cells arising directly from mycelia, monoblastic, cylindrical, hyaline to pale brown. Conidia (17–21 × 8–10 µm) ($\bar{x}$ = 19 × 9 µm, n = 30), ellipsoidal to pyriform, hyaline, with an obliquely prominent truncate basal scar, 2-celled, constricted at the septum, smooth, thick-walled.

Culture characteristics: —Colonies on PDA reaching 40–70 mm diameter after 14 days at 25 °C in darkness. The surface of the colony was pale pinkish-brown, abundant aerial mycelium, grayish pinkish-brown on the reverse. Pale yellow conidiomata are formed after 14 days on PDA.

Material examined: —China, Yunnan Province, Diqing City, Weixi County, 27°00′45.96″ N, 99°21′35.24″ E (2475 m), isolated from healthy leaves of *R. decorum*, September 2024, Z.Y. Huang, B-579 (HKAS 148949), living culture, CGMCC 3.29134 = KUNCC25-19535.

Notes: —Phylogenetic analyses showed that our isolate clustered together with *Trichothecium roseum* (Fig. 4). Morphologically, the isolate closely resembles *T. roseum* (JKL-GFP-22-010) characterized by hyaline, septate, branched conidiophores, and 2-celled, ellipsoidal to pyriform conidia with an obliquely prominent truncate basal scar (Monika & Benjarong 2023). JKL-GFP-22-010 was selected for sequence comparison as it represents a well-documented reference strain of *T. roseum* in a recent taxonomic study (Monika & Benjarong 2023). The ITS and LSU sequences of our strain show 100% similarity with JKL-GFP-22-010.

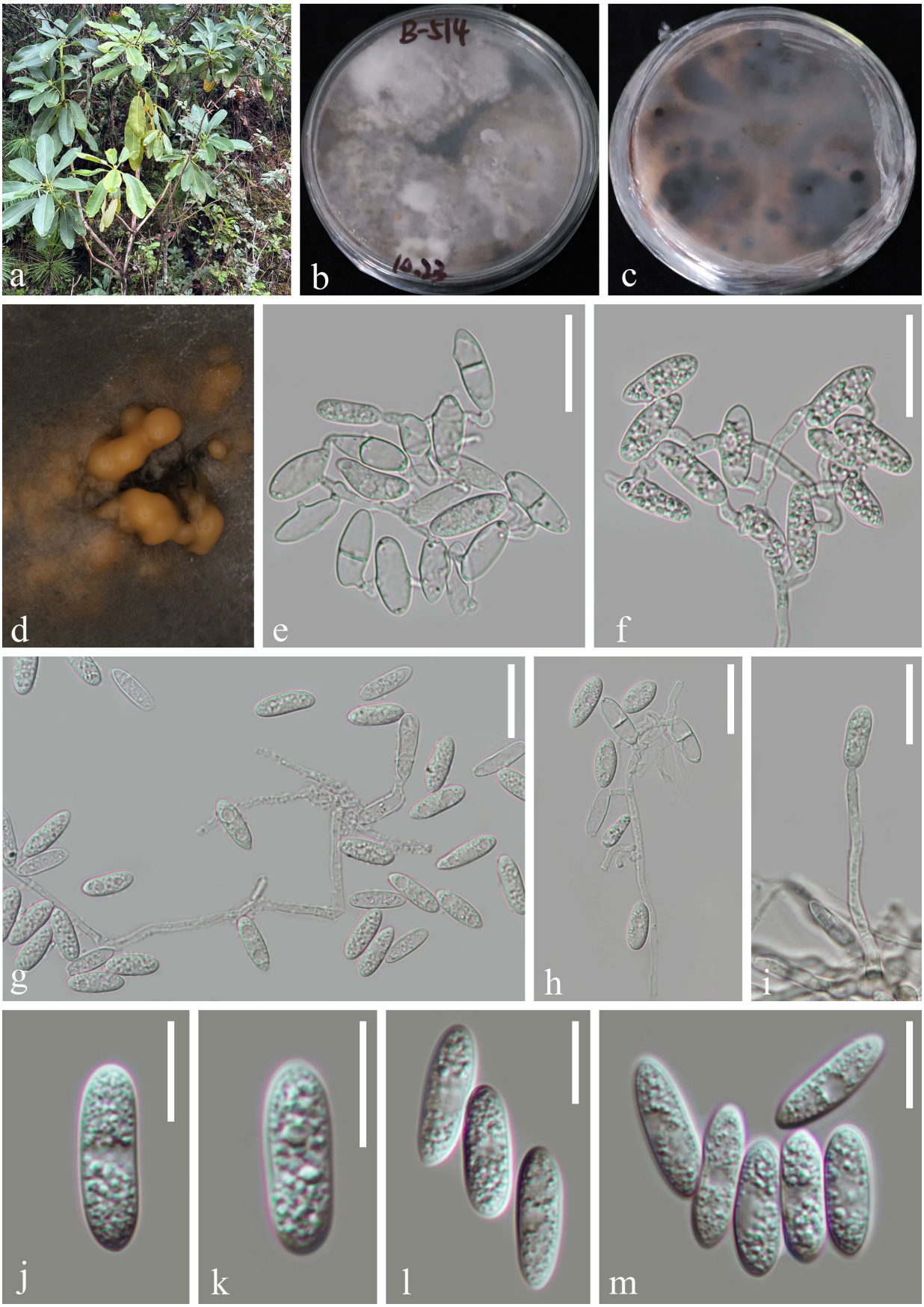

Fig 8. ***Colletotrichum godetiae*** **(HKAS 148951) a.** Leaves of *Rhododendron decorum*. **b, c.** Culture on potato dextrose agar (PDA) (obverse and reverse view). **d.** Conidiomata on PDA. **e–i.** Conidiophores and developing conidia. **j–m.** Conidia. Scale bars: **e-i** = 20 µm, **j–m** = 10 µm.

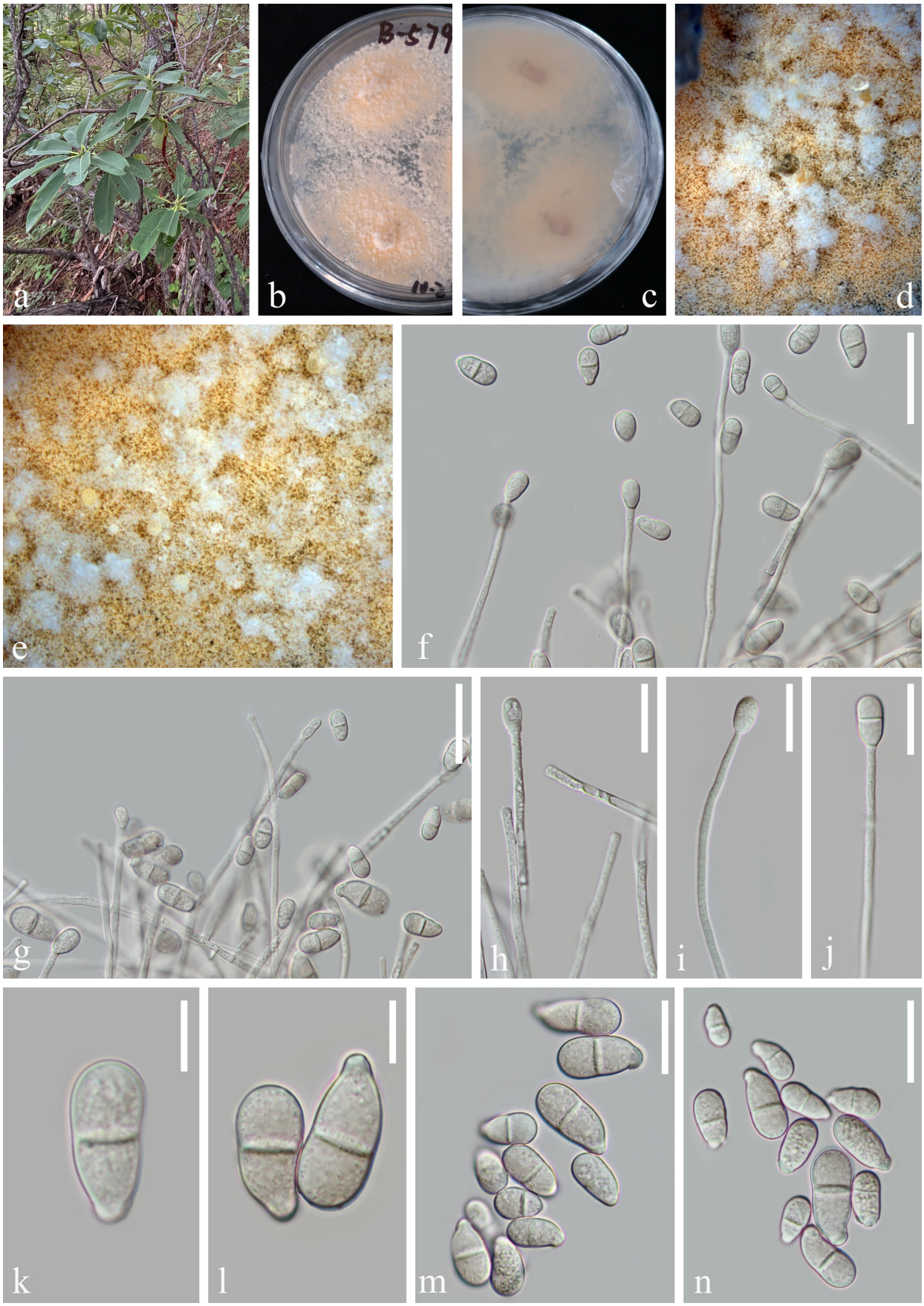

Fig 9. *Trichothecium roseum* (HKAS 148949) a. Leaves of *Rhododendron decorum*. **b, c.** Culture on potato dextrose agar (PDA) (obverse and reverse view). **d, e.** Conidiomata on PDA. **f–j.** Conidiogenous cells and developing conidia. **k–n.** Conidia. Scale bars: **f, g** = 30 µm, **h–j, m, n** = 20 µm, **k, l** = 10 µm.

Discussion

High-altitude plants such as *Rhododendron decorum* are known to harbor a rich diversity of endophytic fungi (Nair & Padmavathy 2014; Rojas-Jiménez et al. 2016; Huang et al. 2024). However, the isolation and morphological identification of these fungi remain particularly challenging due to their inherently slow growth, low sporulation rates, and frequent contamination by epiphytic microorganisms. Following the methods of Tao et al. (2013) and Gu et al. (2022), the effectiveness of surface sterilization was verified by plating aliquots of the final rinse water onto potato dextrose agar (PDA) as negative controls. To minimize contamination by epiphytic microorganisms, leaf discs were subsequently inoculated onto PDA plates supplemented with antibiotics. These results demonstrate that appropriate surface sterilization and the use of antibiotic-supplemented media are effective in reducing contamination during the isolation of endophytic fungi.

Species delimitation of endophytic fungi presents additional challenges, particularly in genera such as *Pestalotiopsis*, *Pezicula*, and *Colletotrichum*, which often exhibit highly similar morphological characteristics, making identification based solely on traditional morphology difficult (Damm et al. 2012; Maharachchikumbura et al. 2014; Bao et al. 2025). In this study, we applied integrative taxonomy by combining detailed morphological observations with multi-locus phylogenetic analyses (Bao et al. 2025), achieving substantial progress in resolving species boundaries. We successfully identified two novel *Pestalotiopsis* species (*P. decori* and *P. jianchuanensis*), one new *Pezicula* species (*P. gaoligongensis*), and reported *C. godetiae* from *R. decorum* for the first time. These findings highlight the remarkable potential of high-altitude plants as valuable reservoirs of fungal diversity. Overall, this study not only reveals the diversity of foliar endophytic fungi associated with *R. decorum*, but also emphasizes the complexity and necessity of microbial resource surveys in extreme ecological environments. Such documentation not only enriches our understanding of fungal taxonomy and systematics but also lays the groundwork for future investigations into plant, microbe interactions and the potential exploitation of these fungi in biotechnology.

Conclusions

Based on multigene phylogenetic analyses and morphological characteristics, five endophytic fungal species associated with *Rhododendron decorum* were identified, including three new species (*Pestalotiopsis decori*, *P. jianchuanensis*, and *Pezicul gaoligongensis*), one new host record (*Colletotrichum godetiae*), and one known species (*Trichothecium roseum*). While the number of species documented in this study is limited, these findings provide preliminary insights into the diversity of foliar endophytic fungi associated with *R. decorum* in high-altitude ecosystems. Further studies with broader sampling are warranted to comprehensively assess species diversity, elucidate ecological functions, and explore the potential roles of these fungi in plant–microbe interactions and high-altitude ecosystem processes.

Acknowledgments

We thank the High-Level Talents Program of Yunnan Province (YNQR-QNRC-2020-113) for the financial support. Zi-Yang Huang thanks Zheng-Quan Zhang, Wen-Peng Wang, and Kai-Yang Niu for sharing morphological and phylogenetic knowledge. Sha Luan, Liang Zhang, and Ying Wang are acknowledged for their help in DNA extraction and PCR amplification. Rong-Ze Ji and Li-Heng Mu are also acknowledged for providing valuable support during sample collection.

Author contributions

Conceptualization, Huang ZY and Luo ZL; methodology, Huang ZY and Shen HW; formal analysis, Huang ZY; resources, Luo ZL; writing—original draft preparation, Huang ZY; writing—review and editing, Shen HW, Huang ZY and Luo ZL; supervision, Luo ZL; funding acquisition, Luo ZL. All authors have read and agreed to the published version of the manuscript.

ORCID

Zi-Yang Huang: https://orcid.org/0009-0007-1284-3995
Zong-Long Luo: https://orcid.org/0000-0001-7307-4885

Conflict of interest statement

The author list includes members of the Editorial Board of PhytoMycology. They were not involved in the journal's review of, or decisions related to, this manuscript. The authors declare no competing interests.

Supplementary Information

The online version contains supplemental information available at https://doi.org/10.65390/phytomyc.2026.2004. Table S1-S4. Strains used in this study and their accession numbers. Newly generated sequences are in red and type strains are in bold.

References

Bao DF, Zhang JY, Lu YZ, Tian XG, Hyde K, Liu N, Xiao Y, Luo Z, Karunarathna S, Samarakoon M et al (2025) Endophytic fungi associated with medicinal ferns in Guizhou Province, China I: Morpho-molecular characterization of culturable endophytic fungi associated with *Dicranopteris* spp. Mycosphere 16(1):2259–2455. https://doi.org/10.5943/mycosphere/16/1/13

Bhat DJ, McKenzie EHC, Bahkali AH, Hyde KD (2012) A multi-locus backbone tree for *Pestalotiopsis*, with a polyphasic characterization of 14 new species. Fungal Diversity 56(1):95–129. https://doi.org/10.1007/s13225-012-0198-1

Capella-Gutiérrez S, Silla-Martínez JM, Gabaldón T (2009) trimAl: A tool for automated alignment trimming in large-scale phylogenetic analyses. Bioinformatics 25(15):1972–1973. https://doi.org/10.1093/bioinformatics/btp348

Carbone I, Kohn LM (1999) A method for designing primer sets for speciation studies in filamentous ascomycetes. Mycologia 91:553–556. https://doi.org/10.1080/00275514.1999.12061051

Chethana KWT, Manawasinghe IS, Hurdeal VG, Bhunjun CS, Appadoo MA, Gentekaki E, Raspé O, Promputtha I, Hyde KD (2021) What are fungal species and how to delineate them? Fungal Diversity 109:1–25.

https://doi.org/10.1007/s13225-021-00483-9

Crous PW, Groenewald JZ, Risède JM, Simoneau P, Hyde KD (2004) *Calonectria* species and their *Cylindrocladium anamorphs*, species with sphaeropedunculate vesicles. Studies in Mycology 50:415–430. https://doi.org/10.3114/sim.55.1.213

Damm U, Cannon PF, Woudenberg JH, Crous PW (2012) The *Colletotrichum acutatum* species complex. Studies in Mycology 73(1):37–113. https://doi.org/10.3114/sim0010

De Silva DD, Crous PW, Ades PK, Hyde KD, Taylor PWJ (2017) Life styles of *Colletotrichum* species and implications for plant biosecurity. Fungal Biology Reviews 31:155–168. https://doi.org/10.1016/j.fbr.2017.05.001

De Silva NI, Brooks S, Lumyong S, Hyde KD (2019) Use of endophytes as biocontrol agents. Fungal Biology Reviews 33:133–148. https://doi.org/10.1016/j.fbr.2018.10.001

Deepak H, Virk V (2022) Optimization of surface sterilization method for the isolation of endophytic fungi associated with *Curcuma longa* L. and their antibacterial activity. Journal of Advanced Biotechnology and Experimental Therapeutics 5(2):334-346. https://doi.org/10.5455/jabet.2022.d119

Fang MY, Fang RC, He MY, Hu LZ et al (2005) *Rhododendron*. Flora China 14:260–455.

Fontana DC, de Paula S, Torres AG, de Souza VHM, Pascholati SF, Schmidt D, Dourado Neto D (2021) Endophytic Fungi: Biological Control and Induced Resistance to Phytopathogens and Abiotic Stresses. Pathogens 10(5):570. https://doi.org/10.3390/pathogens10050570

Gao FK, Dai CC, Liu XZ (2010) Mechanisms of fungal endophytes in plant protection against pathogens. African Journal of Microbiology Research 4(13):1346–1351.

Georgian E, Emshwiller E (2016) *Rhododendron* Uses and Distribution of this Knowledge within Ethnic Groups in Northwest Yunnan Province, China. Open J Soc Sci 4:138-150. https://doi.org/10.4236/jss.2016.41018

Glez-Peña D, Gómez-Blanco D, Reboiro-Jato M, Fdez-Riverola F, Posada D (2010) ALTER: program-oriented conversion of DNA and protein alignments. Nucleic Acids Research 38:W14-W18. https://doi.org/10.1093/nar/gkq321

Gu R, Bao DF, Shen HW, Su XJ, Li YX, Luo ZL (2022) Endophytic *Pestalotiopsis* species associated with *Rhododendron* in Cangshan Mountain, Yunnan Province, China. Frontiers in Microbiology 13:1016782. https://doi.org/10.3389/fmicb.2022.1016782

Hall TA (1999) BioEdit: a user-friendly biological sequence alignment editor and analysis program for Windows 95/98/NT. Nucleic Acids Symposium Series 41:95–98.

Hosking JE, Mesarich CH, Tarallo M, de la Rosa S, Rivera SA (2024) First Report of *Colletotrichum fioriniae* and *Colletotrichum godetiae* causing anthracnose disease of Blueberry (*Vaccinium corymbosum* L.) Fruit in New Zealand. Australasian Plant Pathology 53:503–506. https://doi.org/10.1007/s13313-024-01002-5

Huang ZY, Shen HW, Su XJ, Luo ZL (2024) *Phyllosticta cangshanensis* sp. nov., an endophytic fungus from *Rhododendron decorum* in Cangshan Mountain, Yunnan Province, China. Phytotaxa 678(3):146-166. https://doi.org/10.11646/phytotaxa.678.3.1

Katoh K, Rozewicki J, Yamada KD (2019) MAFFT online service: multiple sequence alignment, interactive sequence choice and visualization. Briefings in Bioinformatics 20:1160–1166. https://doi.org/10.1093/bib/bbx108

Kuraku S, Zmasek CM, Nishimura O, Katoh K (2013) A leaves facilitates on-demand exploration of metazoan gene family trees on MAFFT sequence alignment server with enhanced interactivity. Nucleic Acids Research 41:W22–W28. https://doi.org/10.1093/nar/gkt389

Kusari S, Pandey SP, Spiteller M (2013) Untapped mutualistic paradigms linking host plant and endophytic fungal production of similar bioactive secondary metabolites. Phytochemistry 91:81–87. https://doi.org/10.1016/j.phytochem.2012.07.021

Liu JK, Phookamsak R, Doilom M, Wikee S, Li YM, Ariyawansha H, Boonmee S, Chomnunti P, Dai DQ, Bhat JD et al (2012) Towards a natural classification of Botryosphaeriales. Fungal Diversity 57:149–210. https://doi.org/10.1007/s13225-012-0207-4

Liu YJ, Whelen S, Hall BD (1999) Phylogenetic relationships among ascomycetes: evidence from an RNA polymerse II subunit. Molecular Biology and Evolution 16(12):1799–1808. https://doi.org/10.1093/oxfordjournals.molbev.a026092

Maharachchikumbura SSN, Guo LD, Cai L, Chukeatirote E, Wu WP, Sun X, Crous PW, Bhat DJ, McKenzie EHC, Bahkali AH et al (2012) A multi-locus backbone tree for *Pestalotiopsis*, with a polyphasic characterization of 14 new species. Fungal Diversity 56:95–129. https://doi.org/10.1007/s13225-012-0198-1

Maharachchikumbura SSN, Hyde KD, Groenewald JZ, Xu J, Crous PW (2014) *Pestalotiopsis* revisited. Studies in Mycology 79(1):121–186. https://doi.org/10.1016/j.simyco.2014.09.005

Meena H, Hnamte S, Siddhardha B (2019) Secondary metabolites from endophytic fungi: chemical diversity and application. In: Singh BP (ed) Advances in Endophytic Fungal Research: Present Status and Future Challenges. Springer, Cham, pp 145–169. https://doi.org/10.1007/978-3-030-03589-1_7

Miller MA, Pfeiffer W, Schwartz T (2010) Creating the CIPRES science gateway for inference of large phylogenetic trees. In: Proceedings of the 2010 Gateway Computing Environments Workshop (GCE), November 2010. New Orleans, Louisiana, pp 1–8. https://doi.org/10.1109/GCE.2010.5676129

Monika G, Benjarong KT (2023) First Detection of *Trichothecium roseum* Causing Leaf Spots on Tomato in Germany. Plant Dis 107(4):1233. https://doi.org/10.1094/PDIS-07-22-1588-PDN

Nair DN, Padmavathy S (2014) Impact of endophytic microorganisms on plants, environment and humans. The Scientific World Journal 2014:250693. https://doi.org/10.1155/2014/250693

Nylander JAA (2004) MrModeltest v2 Program distributed by the author. Evolutionary Biology Centre, Uppsala University: Uppsala, Sweden.

Petrini O, Fisher P (1990) Occurrence of fungal endophytes in twigs of *Salix fragilis* and *Quercus robur*. Mycological Research 94:1077–1080. https://doi.org/10.1016/s0953-7562(09)81336-1

Poveda J, Eugui D, Abril-Urías P, Velasco P (2021) Endophytic fungi as direct plant growth promoters for sustainable agricultural production. Symbiosis 85(1):1–19. https://doi.org/10.1007/s13199-021-00789-x

Promputtha I, Lumyong S, Dhanasekaran V, McKenzie EH, Hyde

KD, Jeewon R (2007) A phylogenetic evaluation of whether endophytes become saprotrophs at host senescence. Microbial Ecology 53(4):579–590. https://doi.org/10.1007/s00248-006-9117-x

Rannala B, Yang Z (1996) Probability distribution of molecular evolutionary trees: a new method of phylogenetic inference. Journal of Molecular Evolution 43:304–311. https://doi.org/10.1007/BF02338839

Rathnayaka AR, Tennakoon DS, Jones GE, Wanasinghe DN, Bhat DJ, Priyashantha AKH, Stephenson SL, Tibpromma S, Karunarathna SC (2024) Significance of precise documentation of hosts and geospatial data of fungal collections, with an emphasis on plant-associated fungi. New Zealand Journal of Botany 63(2–3):462–489. https://doi.org/10.1080/0028825X.2024.2381734

Rojas-Jiménez K, Hernández M, Blanco J, Vargas LD, Acosta-Vargas LG, Tamayo G (2016) Richness of cultivable endophytic fungi along an altitudinal gradient in wet forests of Costa Rica. Fungal Ecology 20:124–131. https://doi.org/10.1016/j.funeco.2015.12.006

Ronquist F, Huelsenbeck JP (2003) MrBayes3: bayesian phylogenetic inference under mixed models. Bioinformatics 19:1572–1574. https://doi.org/10.1093/bioinformatics/btg180

Saikkonen K, Faeth SH, Helander M, Sullivan TJ (1998) Fungal endophytes: a continuum of interactions with host plants. Annual Review of Ecology and Systematics 29(1):319–343. https://doi.org/10.1146/annurev.ecolsys.29.1.319

Saikkonen K, Helander M, Faeth SH (2004) Fungal endophytes: hitchhikers of the green world. In: Mukerji KG (ed) Plant Microbiology. Taylor & Francis, London, pp 81–101.

Schardl CL, Craven KD, Speakman S, Stromberg A, Lindstrom A, Yoshida R (2008) A novel test for host-symbiont codivergence indicates ancient origin of fungal endophytes in grasses. Systematic Biology 57(3):483–498. https://doi.org/10.1080/10635150802172184

Shrestha N, Wang Z, Su X, Xu X, Lyu L, Liu Y, Dimitrov D, Kennedy JD, Wang Q, Tang Z et al (2018) Global patterns of *Rhododendron* diversity: The role of evolutionary time and diversification rates. Global Ecology and Biogeography 27:913–924. https://doi.org/10.1111/geb.12750

Stamatakis A (2006) RAxML-VI-HPC: maximum likelihood-based phylogenetic analyses with thousands of taxa and mixed models. Bioinformatics 22:2688–2690. https://doi.org/10.1093/bioinformatics/btl446

Stamatakis A, Hoover P, Rougemont J (2008) A rapid bootstrap algorithm for the RAxML web-servers. Systematic Biology 57:758–771. https://doi.org/10.1080/10635150802429642

Sun H, Zhang J, Deng T, Boufford DE (2017) Origins and evolution of plant diversity in the Hengduan Mountains, China. Plant Diversity 39(4):161–166. https://doi.org/10.1016/j.pld.2017.09.004

Tao G, Liu ZY, Liu F, Gao YH, Cai L (2013) Endophytic *Colletotrichum* species from *Bletilla ochracea* (Orchidaceae), with descriptions of seven new speices. Fungal Diversity 61:139–164. https://doi.org/10.1007/s13225-013-0254-5

Templeton AR, Crandall KA, Sing CF (1992) A cladistic analysis of phenotypic associations with haplotypes inferred from restriction endonuclease mapping and DNA sequence data. III. Cladogram estimation. Genetics 132(2):619–633. https://doi.org/10.1093/genetics/132.2.619

Tian W, Zhang CQ, Qiao P, Milne R (2011) Diversity of culturable ericoid mycorrhizal fungi of *Rhododendron decorum* in Yunnan, China. Mycologia 103(4):703–709. https://doi.org/10.3852/10-296

UNESCO World Heritage Centre (2025) Three Parallel Rivers of Yunnan Protected Areas. UNESCO World Heritage Centre. https://whc.unesco.org/en/list/1083/.

Vilgalys R, Hester M (1990) Rapid genetic identification and mapping of enzymatically amplified ribosomal DNA from several *Cryptococcus* species. Journal of Bacteriology 172(8):4238–4246. https://doi.org/10.1128/jb.172.8.4238-4246.1990

Wang GN, Yu XD, Dong W, Bhat DJ, Boonmee S, Zhang D, Zhang H (2019) Freshwater hyphomycetes in Eurotiomycetes: a new species of *Minimelanolocus* and a new collection of *Thysanorea papuana* (Herpotrichiellaceae). Mycological Progress 18:511–522. https://doi.org/10.1007/s11557-019-01473-7

Wang XQ, Huang Y, Long CL (2013) Assessing the genetic consequences of flower-harvesting in *Rhododendron decorum* Franchet (Ericaceae) using microsatellite markers. Biochemical Systematics and Ecology 50:296–303. https://doi.org/10.1016/j.bse.2013.04.009

White TJ, Bruns T, Lee SJWT, Taylor J (1990) Amplification and direct sequencing of fungal ribosomal RNA genes for phylogenetics. In: Innis MA, Gelfand DH, Sninsky JJ, White TJ (eds) PCR Protocols: A Guide to Methods and Applications. Academic Press, San Diego, pp 315–322. https://doi.org/10.1016/b978-0-12-372180-8.50042-1

Yuan ZL, Verkley GJM (2015) *Pezicula neosporulosa* sp. nov. (Helotiales, Ascomycota), an endophytic fungus associated with *Abies* spp. in China and Europe. Mycoscience 56:205-213. https://doi.org/10.1016/j.myc.2014.06.004

Zhang JH, Li KJ, Liu XF, Yang L, Shen SK (2021) Interspecific Variance of Suitable Habitat Changes for Four Alpine *Rhododendron* Species under Climate Change: Implications for Their Reintroductions. Forests 12(11):1520. https://doi.org/10.3390/f12111520

Zhang YM, Maharachchikumbura SSN, Tian Q, Hyde KD (2013) *Pestalotiopsis* species on ornamental plants in Yunnan province, China. Sydowia 65(1):113–128. https://doi.org/10.1016/j.riam.2013.01.005

Zhao J, Shan T, Mou Y, Zhou L (2011) Plant-derived bioactive compounds produced by endophytic fungi. Mini Reviews in Medicinal Chemistry 11(2):159–168. https://doi.org/10.2174/138955711794519492

Zhu YX, Zhang ZX, Zhang HP, Chai LS, Li L, Ma SG, Li Y (2019) A new ascorbic acid derivative and two new terpenoids from the leaves and twigs of *Rhododendron decorum*. Journal of Asian Natural Products Research 21(6):579–586. https://doi.org/10.1080/10286020.2018.1561669